Solvent Effects on the Electronic Spectra of Transition Metal Complexes

Noel S. Hush*,†,‡ and Jeffrey R. Reimers†,§

School of Chemistry and Department of Biochemistry, University of Sydney, NSW 2006, Australia

Received June 28, 1999

Contents

Noel Hush is an Australian who, after completing undergraduate and Master's studies at the University of Sydney, moved to England to appointments in the Universities of Manchester and Bristol. He returned to Sydney in 1971 to set up a Department of Theoretical Chemistry. He is currently a research professor in the University. His research concerns have ranged rather widely in the areas of molecular structure, excitation, and dynamics. Electron-transfer processes (extending more recently to molecular electronics) have been a particular field of interest.

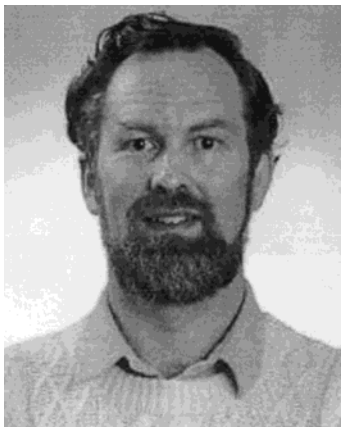

Jeff Reimers received his Ph.D. degree from the Australian National University in 1983 on simulations, with Professor Bob Watts, of the infrared spectrum of water monomer, water clusters, and liquid water. He learned semiclassical techniques for the simulation of condensed-phase spectra during a three-year postdoctoral study at the University of California, San Diego, with Professors Kent Wilson and Eric Heller. Since then he has been an Australian Research Council Research Fellow at the University of Sydney where he has learned electron-transfer theory from Professor Hush. His main interests are in the simulation of molecular spectra, intermolecuar interactions, solvation, photosynthesis, and molecular electronics.

1. Introduction

The method for calculating solvent shifts (i.e., the changes $\Delta\nu$ in the absorption or emission frequency on going from gas phase to solution) on metal-to-ligand charge transfer (MLCT) and other electronic absorption bands involving charge transfer (e.g., ligand to metal, metal to solvent, and organic charge transfer) developed by Zeng, Hush, and Reimers, named ZHR−SS (Zeng−Hush−Reimers solvent shift), is reviewed. The rationale behind ZHR−SS is summarized, as are those of other schemes currently available for the evaluation of solvent effects on electronic spectra. The prognosis for entry into the new millenium is one of optimism concerning semiquantitative predictions and interpretations and one of modified pessimism in relation to precise numerical prediction.

We begin with a brief account of the historical background to solvation theory and shall confine our discussion almost exclusively to water as a solvent, although the methods to be discussed admit of complete generality. The question of the interaction of ions in their ground electronic states with the solvent when dissolved in water solution has a long history, and it is instructive to recall briefly some of the major advances as they contain insights relevant to the much more detailed methods currently in use for excited as well as ground states. All the earlier work was by necessity *analytical*, in contrast to current treatments which involve extensive computa-

* To whom correspondence should be addressed. E-mail: hush_n@chem.usyd.edu.au.
† School of Chemistry.
‡ Department of Biochemistry.
§ E-mail: reimers@chem.usyd.edu.au.

10.1021/cr980409v CCC: $35.00
Published on Web 01/05/2000

tion, and was concerned with monatomic ions. The first important step was taken by Born,[1] who treated ions of charge Z as rigid spheres immersed in a dielectric of static dielectric constant ϵ with effective radius a: the free energy of hydration ΔG was expressed as

$$\Delta G = \frac{Ne^2Z^2}{2a}\left(1 - \frac{1}{\epsilon}\right) \quad (1)$$

where N is Avogadro's constant.

Still within the framework of a continuum model, a number of authors discussed the variation of the solvent dielectric constant induced by the electric field emanating from the ion. Booth,[2] modifying an earlier theory of Kirkwood,[3] calculated the dielectric constant of the solvent in the ion's field as

$$\epsilon = n^2 + \frac{\alpha\pi N_0(n^2+2)\mu}{E} \times L\left[\frac{\beta(N^2+2)\mu E}{2kT}\right] \quad (2)$$

where n is the refractive index of water, N_0 is the number of molecules per unit volume, μ is the dipole moment of a solvent molecule, E is the field strength at the radius of the first coordination sphere, α and β are numerical factors, and L is the Langevin function. Gluckauf[4] used Booth's equation to calculate solvation free energies but with the difference that he allowed for a region of empty space round an ion and between neighboring water molecules in which the dielectric constant falls to unity. This was postulated as a consequence of the mode of packing six water molecules around an ion: in the mathematical treatment, the empty space was averaged into a spherical shell of thickness D which was estimated to be 0.55 Å for alkali ions. This notion of an "effective" radius figures in many subsequent treatments. We shall see later (section 3) that the introduction of an empty shell in the close environment of the ion is also, for somewhat different reasons, a feature of modern theories.

It came to be realized that the continuous dielectric model was too limited in its description of the ion−water interaction, and thus, structural approaches were made. The earliest, and most important, calculation of this type was made by Bernal and Fowler.[5] They included a detailed model of the charge distribution of the water molecules coordinated to the ion, and each water molecule in the first solvation shell of a cation was assumed to bind two further water molecules. The energy of solvation was expressed as the sum of three terms: the ion−dipole interaction for the ion and its nearest neighbors in the coordination shell, the 'Born' energy of solvation of the ion plus its water shell, and the energy of the water molecule which was displaced by the ion. Eley and Evans[6] produced a more detailed version of this approach, as also did Verwey.[7] A number of elaborations followed: that of Buckingham[8] expressed the ion−water interaction as

$$U = U_s + U_t + U_d + U_r \quad (3)$$

where U_s is the electrostatic energy of the permanent multipole moments of water in the field due to the ion, U_t is the energy due to induced multipole moments, and U_d and U_r are contributions from dispersion forces and from electronic repulsion overlap, respectively. The coordination numbers and symmetries were assumed, with the ion lying on the a C_2 axis of the water molecule both for cations and anions. We present simulation studies supporting this assumption later in Figure 2. However, the geometry for anions disagrees with that of Bernal and Fowler, who optimized the energies as a function of ion−molecule distance and angles, and for these it has subsequently been shown that the earlier assignment is substantially correct.

These are the origins of current theories of ion solvation; a succinct account has been given by Case.[9] They all dealt with ions in their ground electronic states and take no account of effects of the solvent's electric field on the ion's electronic structure and hence are unlikely to be appropriate for transition ions with partly filled d-electron shells. Indeed, the ions of the first transition series all have six-coordinate first solvation shells, so that the solution contains $M(H_2O)_6^{z+}$ complexes which themselves are further solvated by additional water molecules. It was first shown by Bethe[10] for neutral ligands with dipole moment μ that the electric field of the coordination shell splits the d-electron levels in ways that depend on the symmetry of the field, thus producing new ground and excited states. This work was rediscovered much later, and the 'crystal field' theory of the spectroscopy of transition ions in water—responsible for the 'renaissance' of inorganic chemistry in the 1960s—emerged (for general references, see Griffith[11]). For a regular octahedral complex, the nonspherical field takes the simple form

$$V_{cf} = K\left(x^4 + y^4 + z^4 - \frac{3\langle r^4\rangle}{5}\right) \quad (4)$$

where the cubic field constant K is given for neutral ligands of dipole moments μ by

$$K = \frac{35e\mu\langle r^4\rangle}{2r^6} \quad (5)$$

where r is the radius of the d-electron shell.

Owing to the high inverse power of the crystal-field potential V_{cf}, the d−d excitations of transition ions in water are essentially the same (except for higher resolution) as those of the corresponding hexaaquo ion in a crystal lattice such as an alum. Thus, only the first coordination shell needs, in general, to be taken into account for consideration of d−d transitions. However, for these complexes in particular and for transition metal complexes in general, there are other important electronic transitions involving electron transfer either to or from the metal and the surrounding ligands. These are generally orders of magnitude more intense than d−d transitions. For these, more extensive solvent effects are very important and to understand them it is necessary to move on from the simpler approaches to take account of the molecular orbital structure of the complex as a whole and consider also a very much more detailed

model of the interaction with the solvent. An example of such a treatment is given for charge-transfer reactions of the $Fe(H_2O)_6^{2+}$ ion in section 5.

If, as with these ligand-to-metal or metal-to-ligand charge-transfer excitations, a significant charge rearrangement is associated with an electronic transition, then in polar media sizable electrostatic interactions between the solute and solvent molecules occur, and these can produce large solvent (solvatochromatic) shifts $\Delta\nu$ of electronic absorption bands. They also modulate the electronic redistribution associated with the transition, as manifested e.g., through observed changes to the transition energy and the induced electron redistribution as reflected in the change in dipole moment $\Delta\mu$ caused by the transition. For a long time there has been much interest in the interpretation of observed solvatochromatic shifts, with earlier models treating the solvent implicitly using a dielectric continuum.[12−18] Indeed, important conclusions concerning the nature of hydrogen bonding were drawn from the results.[19,20] Recently, experimental studies of the change in dipole moment on absorption have become important; these electroabsorption studies were stimulated by the pioneering work of Boxer et al.[21−24] who showed that it is possible to extract intricate details of processes such as electron transfer after photoabsorption within naturally occurring photosynthetic reaction centers as well as MLCT processes in inorganic complexes. Whereas the solvent effect on $\Delta\nu$ amounts to typically only a small fraction of ν itself, the solvent effect on $\Delta\mu$ can be of the same order as the free-molecule value. Interestingly, this work has rekindled research into the effects of polar solutes on the dielectric properties of solvents.[25]

2. Approaches to Treatment of Solvent Effects in Charge-Transfer-Type Excitations

Our aim, in considering solvent effects in charge-transfer-type transitions, has been to develop methods for the quantitative interpretation of the experimental results. This was achieved in two steps: by first modeling the properties of the complexes in the gas phase, and then by modeling the solvent effects on the MLCT transitions. Methods for modeling the solvent effects[26] can be separated into three broad categories: those that treat the solvent implicitly using reaction-field technology, those that consider it in explicit molecular terms, and those that employ statistical mechanical techniques.[27]

Reaction-field techniques[28−34] are extensions of Born's original model, eq 1, and treat the solvent as a dielectric continuum containing a cavity in which the chromophore lies. These methods can qualitatively describe many features of solvation. They can readily be applied to a large range of solvents, but the shape of the solvent cavity is not uniquely defined and the results obtained tend to be very sensitive to assumed cavity shape and size. Modern approaches[34] use prespecified cavity definitions and solve the electronic structure of the chromophore self-consistently with the reaction field generated by the cavity, and these have been very successful. They, however, cannot directly be quantitatively applied in situations in which there are strong specific interactions between the solvent and solute but can be used successfully in supramolecular calculations.[35] Specific solvent interactions result in solvent molecules being placed at specific locations relative to the solute and can even evoke possible chemical effects such as charge transfer with the solvent.[36] Clearly, specific solvation effects could be very important for inorganic complexes (and, in general, for any system involving significant charge transfer), and hence, these approaches were not employed. An example of a reaction-field calculation for MLCT spectral properties is that of Broo and Larsson;[37] while qualitative features are reproduced, issues affecting the method used to describe the solvent (e.g., "cavity radii") impede quantitative analysis.

Methods which involve explicit solvent molecules are usually termed *supramolecular*; there have been a large variety of methods suggested for the implementation of such schemes (see, e.g., refs 36 and 38−44). Two steps are always involved, either implicitly or explicitly: the determination of the solvent structure, and the determination of the (MLCT) spectrum as a function of the solvent structure.

One of the most conceptually appealing schemes for determining the solvent structure is the Carr−Parinello density-functional molecular dynamics scheme (e.g., see ref 45). This determines the solvent structure using a high level of electronic-structure theory, treating all solvent and solute molecules equivalently. Of course, the disadvantage of this approach is the enormous amount of computational resources required, and such schemes are not currently feasible for the study of MLCT spectra.

A variety of more-approximate schemes have been generated, the most promising of which include Warshel's generalized solvation models,[46] hybrid quantum-mechanics/molecular mechanics (QM/MM) schemes,[40,43] and even simpler simulation methods.[47] These treat the chromophore and critical solvent molecules using a high level of theory and the peripheral solvent molecules using more approximate schemes. A scheme of this type has been applied by Zerner to study inorganic MLCT[36] and other[28,29] transitions. This places the solute and a small number of solvent molecules inside a solvent cavity. It has the advantage that it includes all interactions (including charge transfer and dispersion) between the solvent and solute, but the implementation has been restricted by the need to employ the semiempirical INDO technique to describe hydrogen-bonding interactions, for which it is not appropriate,[48] and has been restricted to structures at 0 K.

We choose not to follow these schemes largely because preliminary calculations indicated that the results were unreliable in that the errors arising from the approximations used to solve the electronic structure could not be controlled. Instead, we developed a simpler model, abbreviated ZHR−SS, which will be outlined.

Because of hydrogen bonding and other specific interactions, in quantitative calculations the solvation of the complex must itself be treated in a molecular fashion. A qualitative analytical theory for

the gas-phase to solution-phase frequency change $\Delta\nu$ can be derived for the case in which the solvent is treated as a dielectric continuum with dielectric constant ϵ and refractive index n in which a nonionic chromophore resides inside a spherical cavity of radius a. Methods of this type were developed by McRae and others[12−14,16] and described in the most general form by Liptay,[17] with the most relevant features extracted by Rettig.[18] The most important contributions to the solvent shift are

$$\Delta\nu = -\frac{2\epsilon - 2}{2\epsilon + 1}\frac{1}{a^3}\boldsymbol{\mu}\Delta\boldsymbol{\mu} - \frac{n^2 - 1}{2n^2 + 1}\frac{1}{a^3}|\Delta\boldsymbol{\mu}|^2 \quad (6)$$

The first term is usually the largest in magnitude since $|\boldsymbol{\mu}|$ (the initial-state dipole moment) is often much greater than the dipole change accompanying the transition $|\Delta\boldsymbol{\mu}|$, and for polar solvents, its prefactor is up to 5 times larger. The second term in fact arises from the electronic polarization of the solvent adjusting synchronously with the electronic redistribution which occurs in the chromophore; recently,[49] it has been suggested that it is appropriate to use different cavity radii a for these two terms. Earlier expressions differ from eq 6 in that they introduce crude approximations for the chromophore's polarizability, but general expressions containing $\Delta\alpha$ are available.[17,18] For ionic chromophores, the general picture remains but additional terms must be considered which describe the polarization of the solvent by the ion. The ground-state dipole moment $\boldsymbol{\mu}$ becomes origin dependent, however, and one must proceed cautiously.

3. The ZHR–SS Computational Model for Solvent Effects on MLCT Spectra

The ZHR−SS method comprises four independent steps, with the results of each step being independently verifiable by comparison of the results with experimental data. In this way, computation of (for example) the solvent effects on a MLCT band are not performed in isolation but arise as one element of a broad-ranging model for the spectroscopic, electronic, and geometric properties of the chromophore and the solution. Briefly, the steps involve (1) determining the electronic structure and spectroscopy of the chromophore in the gas phase; (2) determining force fields through which the chromophore interacts with the solvent; (3) determining the structure of the solution; and (4) determining the effect of the solvent structure on the electronic transition of the chromophore.

We find that, in general, only when the electronic structure of the chromophore in its ground electronic state in the gas phase is correctly described is it possible to generate an accurate force field which can predict known properties of the solution, and only when the solution structure is correctly described can the solvent effects on the chromophore be reliably obtained. A subtle but important feature that emerged[48,50] is that solvation also effects the geometry of a complex, and it is important that step 1 be performed at a realistic solution-phase geometry.

While our method embodies a variety of options concerned primarily with choice of electronic structure method, the specification of the intermolecular potential functions, and technical issues such as the choice of boundary conditions used in the computer simulations and while it requires the determination of a significant number of properties of the solvent and solute molecules in the gas phase, it contains no parameters which can *arbitrarily* be adjusted in order to fit experimental spectroscopic data.

To generate a reliable, quantitative scheme for estimating MLCT solvent effects, we consider the metal and all of its ligands as forming the chromophore and treat this in the gas phase using the highest possible level of ab initio calculation. It is then surrounded by a large number (i.e., 100−200) of explicitly represented solvent molecules, and this is then surrounded by small exclusion zone[51] of width r_e and then by a dielectric continuum of radius a. This is illustrated in Figure 1; we use a value of 1 Å for r_e

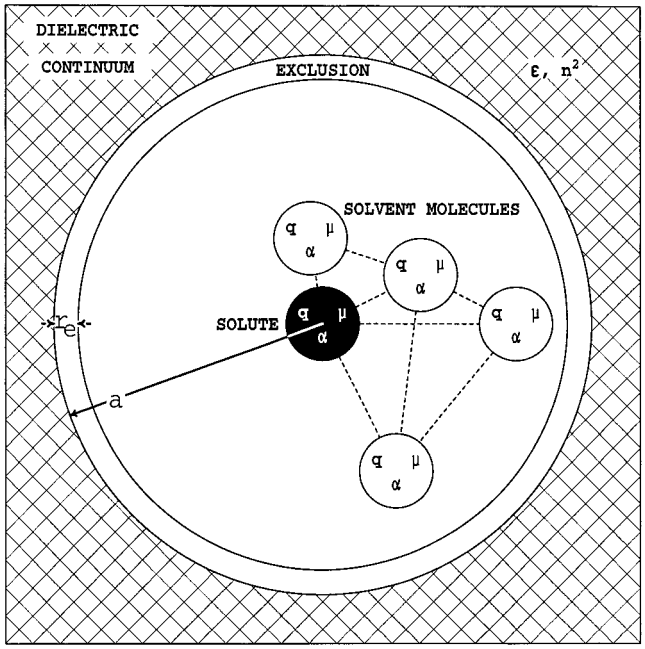

Figure 1. Key physical features of the calculation of the gas-phase to solution solvent shift $\Delta\nu$ and associated properties, averaged over equilibrated liquid configurations. (1) The chromophore (in black) is represented by a set of electronic-state-dependent charges q, permanent and induced point dipoles μ, and polarizability centers α. (2) Some (of typically 100−200) individually represented solvent molecules (in white), similarly described with the permanent moments and charges are electronic state independent; only the induced moments are able to respond to optically induced changes in the chromophore's electronic state. (3) A small exclusion zone of width r_e. (4) An outer dielectric continuum of radius a, dielectric constant ϵ, and refractive index n. The dashed lines indicate some of the specific intermolecular electrostatic interactions.

in all calculations, and typically the largest values of a that are considered are on the order of 9.5−12 Å. For ruthenium ammine complexes, there is no ambiguity concerning, in aqueous solution, which molecules are "ligands" and which are "solvent"; for other problems such as the solvation of Fe(II) in water,[52] however, the inner six water molecules are

taken to form part of an $Fe^{2+}(H_2O)_6$ complex while the *solvent* water molecules are taken to include only waters beyond this ligand shell. This approach is valid provided that inner-shell ligand-exchange reactions are sufficiently slow.

In principle, the inner layer of explicitly represented solvent molecules are presumed to account for all of the specific interactions between the solvent and solute while the dielectric continuum is presumed to account for possible long-range charge−dipole interactions. From the point of view of practicability of calculation, such a separation is at present more or less obligatory, since for ionic solutes the long-range interactions extend over greater lengths than will, for a long time, be possible to include in computer simulations. The dielectric cavity is taken to be spherical in shape with radius *a* which may be set to any value up to the sum of r_e and the inscribed radius of the unit cell used in the liquid simulations. In effect, *a* is not an arbitrary parameter as in practice it is chosen sufficiently large such that the solvent shift is actually insensitive to its value. Results obtained for aqueous solvent shifts of (n,π^*) transitions in pyrimidine[53] as well as for MLCT transitions in $Fe^{2+}(H_2O)_6$[52] and $Ru^{2+}(NH_3)_5$−pyridine[54] are shown in Figure 2 and clearly indicate this.

In practice, we have found[52−54] that effects caused by the specific ordering of solvent molecules in the second and third solvent shells away from the chromophore can be quite large. As a consequence, at radii *a* sufficiently large to include these specific solvation effects, all contributions from the long-range dielectric become insignificant. Hence, in hindsight, inclusion of the long-range contribution often appears to be unnecessary.

The mathematics necessary to describe the dielectric continuum is described in detail elsewhere,[53] but in essence it involves the use of Friedman image technology[55] with spherical boundary conditions. The equilibrated chromophore in its initial electronic state polarizes the dielectric continuum via image charges and dipoles embedded within it. Standard analytical limits such as eq 6, or close approximations thereto, are retrieved in a variety of limits[53] for both ionic and nonionic chromophores.

ZHR−SS involves two major stages: the generation of representative structures for the solution and the evaluation of the solvent effects based on those structures. Any available technique may be used for the first stage, provided that it gives reliable results. We usually perform classical simulations employing effective pair potentials derived[56] using the scheme of Kollman,[57−60] these being rigid-molecule Monte Carlo simulations with the geometry of the complex taken to represent the geometry in solution as accurately as possible. The intermolecular potential functions are generated by combining a standard set of Lennard−Jones potentials with intermolecular electrostatic interactions individually calculated for each isolated chromophore molecule in its initial electronic state (the ground state for an absorption experiment but the excited state for an emission experiment). While potential functions of this type are cumbersome to evaluate compared to canned potential functions, they offer the advantages of

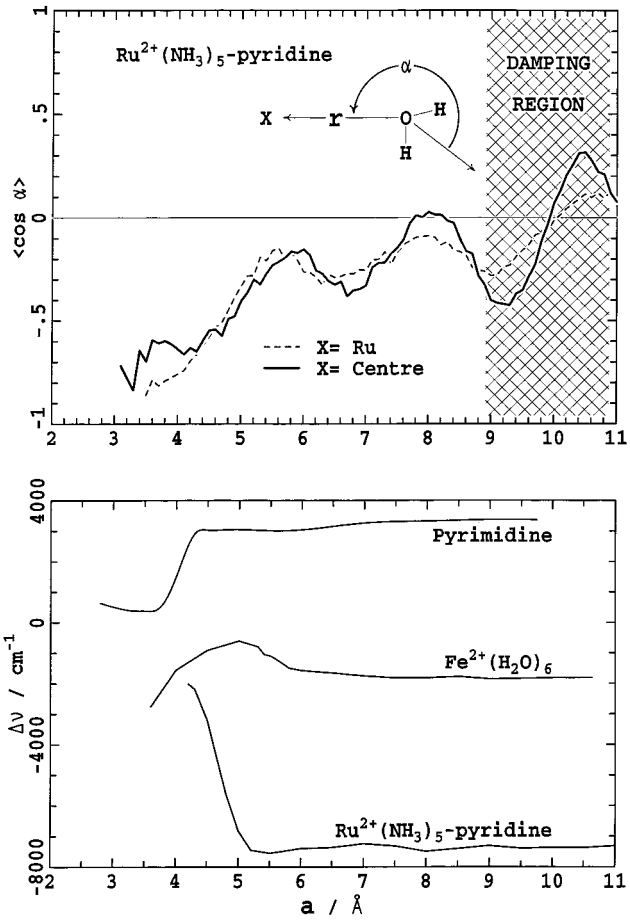

Figure 2. The lower frame shows ZHR−SS calculated gas-phase to aqueous solution solvent shifts $\Delta\nu$ as a function of the dielectric cavity radius *a* for the lowest (n,π^*) band of pyrimidine,[53] for the ultraviolet photoionization band of $Fe^{2+}(H_2O)_6$,[52] and for the visible MLCT band of $Ru^{2+}(NH_3)_5$−pyridine,[54] illustrating the insensitivity of $\Delta\nu$ to the precise number of explicitly included water molecules. The upper frame shows the calculated angular distribution function $\langle\cos\alpha\rangle$ for $Ru^{2+}(NH_3)_5$−pyridine evaluated by damping to zero the long-range Coulomb interactions over the indicated region as a function of the separation *r*.

greater (and tailorable) accuracy as well as the flexibility to handle excited states. Also, to treat the solvent shift reliably, one must first be able to treat the gas-phase spectroscopy reliably, and so the task of determining the chromophore's electronic structure is one which in any case must be completed.

The Lennard−Jones terms used in Kollman's potentials are designed to accompany atomic charges for the solute determined at the ab initio Hartree−Fock self-consistent-field (SCF) level by fitting atomic charges to the molecular electrostatic potential (ESP) outside the molecular van der Waals shell. We have found that this approach gives reasonable results provided that the electronic structure of the solute is properly described at the SCF level. Use of potentials obtained using higher levels of theory, e.g., using multiconfigurational SCF (MCSCF), also produce liquid structures that are qualitatively reasonable but overestimate the hydrogen-bond strength and are quantitatively inferior. Clearly, a revised set of Lennard−Jones parameters optimized for use with more-accurate solute charge distributions is war-

ranted but at this stage is unavailable. Indeed, often the SCF electronic structure is qualitatively flawed, making employment of more-accurate charge distributions essential.[61] This aspect of our approach constitutes a weakness in that it is not a simple black-box technique in which you dial-up the system and obtain the answer. On the other hand, the final solution to any problem will appear well-founded as it must simultaneously reproduce a large amount of experimental information ranging from the gas-phase structure of the chromophore to cluster data and the nature of intermolecular interactions to the liquid structure to the effects of solvation. Each of the key steps are essentially individually assessable; each has its own assessment criteria, and modifications can be introuced until satisfactory results are obtained.

In the second major stage of ZHR−SS, sampled liquid configurations are processed in order to determine the solvent shift of the absorption band. It is assumed that a significant charge redistribution occurs as the result of the electronic transition and that the solvent shift arises from the changes in the electrostatic interactions between the solvent and solute (this method is thus clearly inappropriate for the study of d → d transitions as these involve essentially no macroscopic charge redistribution[62]). The effects of the solvent on the electronic structure of the solute, and vice versa, are included by treating each molecule as being individually polarizable. This is tantamount to taking the electronic structure of the supramolecular assembly and expressing it self-consistently in terms of a perturbation expansion based on the electronic structures of the individual molecules. The varying properties used to describe the chromophore, the individually represented water molecules, and the dielectric continuum are all depicted in Figure 1.

The above treatment of polarization is only valid if the perturbation expansion converges quickly. We investigated[48] one complex, $Ru(II)(NH_3)_5$−pyrazine-H^+, in which two molecular orbitals come into resonance; if such a resonance is established by the intermolecular interactions, then a perturbation expansion based on the gas-phase properties would not converge and the electronic structure of the chromophore and solute must then be determined together by ab initio means. For $Ru(II)(NH_3)_5$−pyrazine-H^+, however, the resonance was in fact found to be a gas-phase property and the perturbation expansion remained rapidly convergent.

Charge transfer between the chromophore and solvent molecules is not automatically included but could be explicitly included in ZHR−SS if necessary. Test ab initio calculations[53] indicate, however, that solvent effects can be extremely sensitive to small amounts of charge transfer and that semiempirical methods such as INDO represent intermolecular charge-transfer and hence solvent effects derived from it rather poorly. While solvent-shift calculations using methods such as INDO have been performed,[28,29,36] we feel that at present the most reliable method currently available for treating charge-transfer effects is to neglect them completely. The results which we have obtained so far (shown in Table 2) indicate that while there could possibly be a significant (of order 10%) charge-transfer solvent effect on $\Delta\mu$, this contribution is clearly not dominant.

The physical effects on an electronic transition induced by solvation included in ZHR−SS can be summarized: the solvent is initially polarized in equilibrium with the chromophore in its initial electronic state; when the chromophore jumps to its final electronic state, the component of the solvent's polarization attributed to solvent alignment remains fixed and interacts with the chromophore's electronic redistribution while the component attributed to electronic polarization of the solvent is allowed to reequilibrate with the chromophore's new electronic structure. Dispersion interactions, believed to contribute on the order of 300 cm^{-1} to most solvent shifts, are not included.

4. Calculations for Azine Solutions Using the ZHR–SS Method

ZHR−SS is expected to be applicable for any system involving charge transfer. Before considering MLCT reactions, we first considered (n,π*) spectra in azines in which an electron is removed from a nitrogen lone-pair orbital and transferred to the π LUMO orbital. Compared to MLCT transitions, the electron moves a smaller distance and hence the effects are weaker and more difficult to model. Molecules such as these also occur as ligands in transition metal complexes.

These calculations were performed over several years and involve the use of different electronic structure methods for determining the gas-phase properties of the chromophores. This variety arose from a combination of factors ranging from technical feasibility limits to the need to get the electronic structure qualitatively correct. A total of 102 solvent molecules are used in each simulation, however, allowing for a maximum dielectric radius $a \approx 9.5$ Å. Key results for the calculated absorption and fluorescence solvent shifts, $\Delta\nu_A$ and $\Delta\nu_F$, respectively, and for the enthalpy of hydration ΔH are summarized in Table 1. The enthalpies of hydration are systematically too large, especially if post-SCF methods are employed to generate the atomic charges for use in the intermolecular potential functions, and the calculated solvent shifts (using no arbitrarily adjustable

Table 1. Solvent Shifts for Azines in Aqueous Solution[a]

		$\Delta\nu$ (absorption)		$\Delta\nu$ (fluorescence)		ΔH	
azine	method[b]	calcd	obsd	calcd	obsd	calcd ± 2	obsd[c]
pyridine[d]	SCF	3500	>2500			−13.6	−11.9
pyridazine[e]	CASSCF	4100	3800	800	700	−18.5[h]	−14.9
pyrimidine[f]	SCF	3400	2700	−300	−600	−16.9	−14.3
pyrazine[g]	MRCI	2000	1800	300	700	−16.2[i]	−11.8

[a] Gas-phase to aqueous solution solvent shifts $\Delta\nu$ are in cm^{-1}, while enthalpies of hydration ΔH are in kcal mol^{-1}; the method is that as used to calculate the gas-phase electronic structure of the chromophore. [b] The method used to determine the energetic and electrostatic properties of the chromophore in the gas phase. [c] Reference 77. [d] Reference 71. [e] Reference 64. [f] References 53 and 56. [g] Reference 61. [h,i] If an SCF-derived pyridazine−water intermolecular potential is used, values of −16.1 and −13.5 kcal mol^{-1} using SCF-derived potentials are obtained, respectively.

parameters) are accurate to ±700 cm^{-1}. While 700 cm^{-1} is significantly large for the azines, it is on the order of expected contributions from dispersion effects and is small compared to solvent shifts expected for inorganic MLCT spectra. As detailed individually,[53,61,63,64] the calculations do describe a large range of other experimental data adequately, ranging from solution properties to properties of hydrogen-bonded dimeric complexes to high-resolution gas-phase spectroscopic properties of the chromophores. Further, the solvent-shift results are sufficiently accurate to discriminate between various current models for the electronic structures of the azines. For example, the lone pairs in pyrazine have traditionally been described as noninteracting, with (n,π^*) excitation localizing on just one of them (the issue of localized versus delocalized excitations here closely parallels well-known issues in the spectroscopy of inorganic complexes such as the Creutz−Taube ion[65]). This model was based on the interpretation (in the spirit of eq 6) of solvent-shift data and on results of SCF and valence-bond electronic structure calculations. An error[61] of interpretation in the original experimental paper[15] resulted in the observed fluorescence solvent shift being seen to be compatible with a localized description while the observed absorption solvent shift demanded this description. ZHR−SS results,[61] to the contrary, show that the observed absorption shift is compatible with either model while the observed fluorescence shift demands a delocalized model. We showed that only a delocalized model is compatible with the observed gas-phase high-resolution spectra and that inclusion of dynamic correlation in extensive complete-active-space self-consistent-field (CASSCF) calculations with multireference configuration interaction (MRCI) predicts a delocalized structure in the gas phase. Calculated potential-energy surfaces obtained using this and simpler techniques are shown in Figure 3, along with the

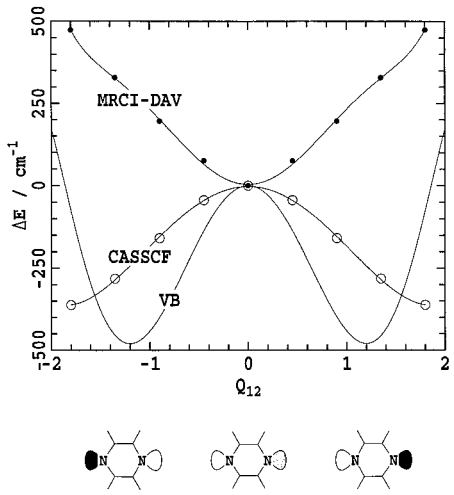

Figure 3. Potential-energy surfaces for the first (n,π^*) singlet excited state of free molecular pyrazine evaluated using CASSCF and Davidson-corrected MRCI methods[61] and with valence-bond methods[78] methods. The structures show, in particular, the change in the CNC bond angles as the molecule distorts an amount Q_{12} in the direction of the (dimensionless) antisymmetric normal mode ν_{12}, the shaded areas reflecting zero (white), half (gray), and full (black) occupancy of the nitrogen lone-pair orbital.

calculated pyrazine geometries at the stationary points. Further, we estimated values for the effective coupling J and the reorganization energy and showed that additional solvent contributions to the reorganization energy were not of the correct magnitude to localize the excitation in solution.

5. Results from ZHR–SS for MLCT Transitions in Ru Complexes

We have studied solvation and solvation effects on MLCT processes in complexes $Ru^{2+}(NH_3)_5$−L, with L = pyridine, pyrazine, pyrazine-H^+, and NH_3 using ab initio MCSCF methods to describe the gas-phase electronic structure of the complexes. Key results for the hydrogen bonding, frequency shift $\Delta\nu$, and change in $\Delta\mu$ are shown in Table 2, while hydrogen-bonding and metal−oxygen radial distribution functions are shown in Figure 4. In all simulations, a total of 256 water molecules were included, allowing for a maximum dielectric radius of $a \approx 12$ Å.

The results for the liquid structure indicate that each ammonia hydrogen is hydrogen bonded to one water oxygen. Sometimes one water molecule forms two hydrogen bonds with different ammonia hydrogens so that the total number of water molecules solvating the ammonias is 13 for the hexammine complex and 10−11 for the pentammine complexes. Figure 4 shows that the most probable radius of this first water coordination shell around the ammonias from the metal is ca. 4 Å, as observed experimentally.[54] As neat water itself has its second coordination shell at approximately this radius containing 12 water molecules, the density of water molecules near the ion is similar to that of bulk density. This, plus the similarity of the radial distribution functions in Figure 4 with those for pure water (the TIP3P water potential[66] is used throughout), suggests that the water molecules around the complex do not have enhanced hydrogen bonding or other properties. Such enhancement could be produced through charge-transfer or polarization effects, however, which are not included in these simulations.

Around azine ligands L, no hydrogen bonding is calculated for L = pyridine, one hydrogen bond is calculated to form to the free nitrogen for L = pyrazine, and almost two hydrogen bonds are calculated to form to the acidic hydrogen for L = pyrazine-H^+. This result for L = pyridine is as expected, but those for L = pyrazine differ somewhat from the results of alternate simulations. Using a molecular mechanics potential, Broo[67] found no hydrogen bonding to pyrazine ligand. These simulations considerably overestimate the separation of the water molecules hydrogen bonded to ammonia (the Ru−O distance is predicted to be ca. 5 Å instead of the observed value of ca. 4 Å), and analogous potentials for pyrazine in water also predict no hydrogen bonding, contrary to experiment. It seems that simple molecular-mechanics-type potential functions are not sufficiently flexible to describe correctly the hydrogen-bonding interactions in these systems. Also, X-α density-functional calculations by Zhang and Ondrechen[68] predict little charge build-up on the free nitrogen, and simulations using their calculated

Table 2. Solvent Effects for Complexes $Ru^{2+}(NH_3)_5-L$ in Aqueous Solution[a]

				ν (soln)			$\Delta\mu$ (soln)					
L	method[b]	ν (gas)	$\Delta\nu$	calcd	obsd	$\Delta\mu$ (gas)	calcd	obsd[c]	obsd[d]	# HB per H from NH_3	# HB H_2O to NH_3	# HB to L
NH_3[e]	MCSCF									1.0	13	
pyridine[e,f]	MCSCF	38	−8	30	24.5	6[h]	5[h]		3.4	0.9	11	0.0
pyrazine[g]	MCSCF	32.6	−8.3	24.3	21.2	8.8	5.5	4.8 ± 1.3	3.5	0.9	10	1.2
pyrazine-H^+ [g]	MCSCF	24.8	−0.5	24.3	18.9	1.0	0.3	<0.3	<1	1.0	10	1.8

[a] Gas-phase to aqueous solution solvent shifts $\Delta\nu$ in are in 1000 cm^{-1}, the changes in dipole on excitation, $\Delta\mu$ are in D, # HB are the number of hydrogen bonds per ammonia hydrogen, the total number of water molecules hydrogen-bonded to ammonias, and the number of water molecules hydrogen bonded to an azine ligand L. [b] Used to determine the energetic and electrostatic properties of the chromophore in the gas phase. [c] Reference 22 in 50% glycerol−water glass. [d] Reference 70 in 50% glycerol−water glass. [e] Reference 54. [f] Reference 50. [g] Reference 48. [h] Estimated by applying an INDO/S derived geometry-relaxation correction to MCSCF results obtained at the calculated gas-phase geometry.

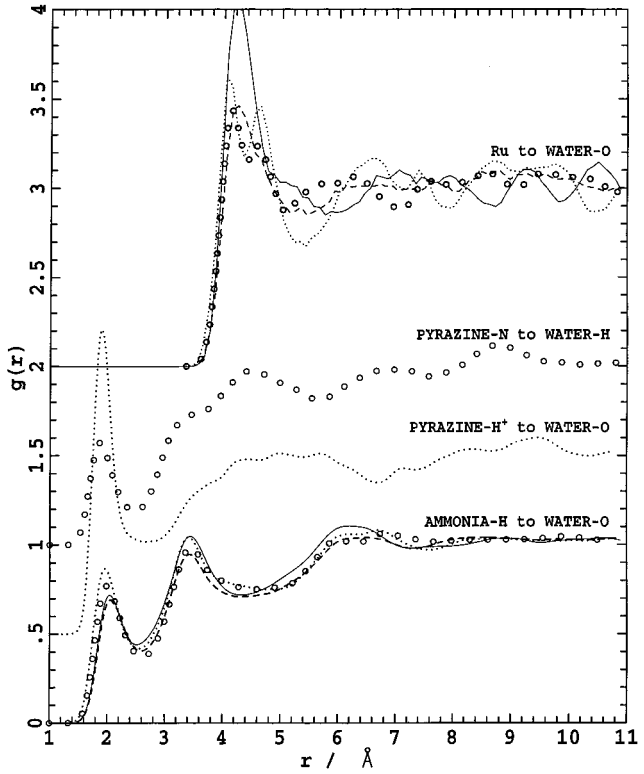

Figure 4. Intermolecular radial distribution functions $g(r)$ showing hydrogen bonding between the inorganic complexes $Ru^{2+}(NH_3)_5-L$ and neighboring waters, for L = NH_3 (—),[54] pyridine (- - -),[54] pyrazine (○),[48] and pyrazine-H^+ (···),[48] as well as the corresponding metal to water-oxygen distributions.

electronic structure for the complex would very likely also predict no hydrogen bonding. Their results seem inconsistent with the observed increase in basicity of the complex with respect to free pyrazine,[54] and again, we see that we must have an accurate description of the electronic structure of the solute before we can consider questions concerning solvation.

For L = pyrazine-H^+, one weak and one strong hydrogen bond are predicted to form to the acidic hydrogen atom. No information is available to ascertain the accuracy of this prediction. Naively, one normally expects only one hydrogen bond per hydrogen atom, but this result may be plausible as this hydrogen does bear a substantial charge which could induce multiple solvation.

For charged systems, the calculated radial distribution functions are quite sensitive to the boundary conditions used in the simulation[52,54] and care must be taken to obtain sensible results. The structural properties which we have found to be the most sensitive are the angular distribution functions which depict the orientation of the water molecules around the ion. An example of this is shown in Figure 2, where the cosine of the angle α between the symmetry axis of a water molecule and the vector between either the metal atom or the solute center of mass and the water oxygen is averaged as a function of the oxygen−metal separation. At short distances, $\langle\cos\alpha\rangle \approx -1$, indicating that the water hydrogens are pointing as much as possible away from the metal. This correlation disappears at intermediate separations (i.e., 8 Å) but reappears near the edge of the simulation cell. In the simulation shown, the long-range Coulomb potentials were damped smoothly to zero over the last 2 Å inside the inscribed radius of the unit cell used in the simulations, and it is precisely in this region that the angular correlation reappears. Use of more sophisticated methods for treating the boundary conditions, such as Ewald summations with neutralizing backgrounds,[54] does not produce this anomaly, but the procedure is computationally prohibitive. This boundary effect will have significant consequences for calculated solvent shifts if the incorrectly orientated water molecules lie close enough to the chromophore. Figure 2 also shows the solvent shift for this system evaluated using a continuum dielectric of radius *a* to replace the outermost water molecules. The results show that the calculated solvent shift has converged to its infinite-radius limit well before anomalies appear in the calculated angular distribution functions. Hence boundary-condition effects are not observed to alter the calculated solvent shift.

For MLCT transitions, no gas-phase spectra are available and hence only the final solvent-corrected values may be compared directly with experiment. Accurate calculation of the gas-phase values is itself not a simple task, with methods such as SCF followed by single and doubles configuration interaction (SDCI) predicting[52] transition energies in error by ca. 50 000 cm^{-1}. MCSCF calculations provide the simplest ab initio computational scheme which provides a qualitatively correct description of electronic structures of ground and excited MLCT states, and it is difficult at this stage to estimate absolute reliabilities for computed quantities. The final calculated solution transition frequencies shown in Table 2 are within

6000 cm^{-1} of the observed values, and of the total, ca. −8000 cm^{-1} is attributed to solvent shift for L = pyrazine and pyridine and almost none for L = pyrazine-H^+. The result for pyrazine-H^+ is consistent with the observed lack of solvent effect on the transition energy and arises from a resonance between the metal d_π orbital and the ligand's LUMO orbital.[69] Certainly, an error of 5000 cm^{-1} in the ab initio calculation of the gas-phase transition energy is quite plausible, and so it is difficult to draw conclusions as to the accuracy of the calculated ca. 8000 cm^{-1} solvent shifts, but based on the results for our test calculations described in section 5, an error of more than 25% (2000 cm^{-1}) would seem improbable.

The final calculated solution dipole moment changes $\Delta\mu$ shown in Table 2 for L = pyrazine and pyridine are within 2 D of the observed values and depict an effective electron-transfer distance r of only one-third of the separation r_0 between the metal and ligand center. This error is ca. 10% of the naive value assuming $r = r_0$ and appears reasonable given the nature of the calculations involved. Also, difficulties exist in the interpretation of the experimental results due to the need to estimate local-field correction factors. Boxer's results[22] include conservative error bars, while Shin et al.[70] have employed some simplistic assumptions in an attempt to reduce this uncertainty. It is certainly possible that the differences between the computed and observed values of $\Delta\mu$ arise in whole or in part from uncertainties in the experimental rather than the computed quantities.

We have shown[50,52,54] that INDO/S provides results of comparable accuracy to the ab initio MCSCF results for the gas-phase transition properties and may be effectively used in this capacity. A modification of the standard INDO/S procedure is necessary, however,[50,54] in that the effects of the electronic redistribution associated with MLCT cannot be treated correctly using an empirical parametrization but must be treated explicitly using MCSCF-MRCI techniques. Alternatively, we have found that INDO/S ground-state electronic wave functions are not sufficiently accurate for the reliable generation of solvent structures.[48,50,52−54,56,61,63,64,71]

6. Photochemistry of $Fe(H_2O)_6^{2+}$ in Water

The spectroscopy and associated chemistry of the hydrated ferrous ion in the ultraviolet region was the subject of continued experimental investigation over three decades, until the topic was more or less abandoned as too difficult in the mid-1960s.[52] The main reason for this interest is that irradiation leads to hydrogen evolution, and the primary photochemical step was an obvious focus of attention. It was of interest to see whether our methods could provide insight into its nature.

Many computer simulations had already been performed on the structure of aqueous Fe(II), and these provided a framework in which we could test ZHR−SS ground-state predictions. As for the Ru(II) complexes discussed in the last section, the simulation of inorganic complexes in water is hampered by various technical problems associated with the presence of ions and the long-range Coulomb forces involved, forces of much longer range than can, at present, be accommodated in simulations using even the simplest potential functions. We demonstrated[52] that intermolecular potential functions obtained using Kollman's scheme[57−60] treating the ion and its inner coordination shell as a single entity adequately reproduce all experimental and theoretical data available. We also simulated aqueous $Ru^{2+}(NH_3)_6$[52] and were able to account for all known experimental data for the structure of this solution.

The ultraviolet electronic absorption spectrum of aqueous Fe(II) has never been assigned, despite extended intense research effort. The transition starts at ca. 40 000 cm^{-1} and appears to reach a maximum near 50 000 cm^{-1} with an extinction coefficient of just 16 L mol^{-1} cm^{-1}, but the remainder of the band (in the vacuum UV) is not yet observed. We considered three of the four generally suggested mechanisms leading to this absorption and were able to conclude from solvent-shift analysis that it does not arise from iron to ligand-water MLCT or from metal 3d → 4s absorption, thus excluding two of these. One of the remaining proposed mechanisms, however, involves direct transfer of an electron from the metal to a preexisting cavity located within the solvent. Treating the gas-phase process as the photodetachment of an electron from Fe^{2+}, a process observed at $\nu = 250\,000$ cm^{-1}, we calculated a solvent shift of −240 000 cm^{-1} and an electron confinement kinetic energy of 40 000 cm^{-1}, thus predicting a transition energy at 50 000 cm^{-1}, as observed. Despite this confinement-energy calculation being very crude, we see that the calculated solvation energy is clearly representative of the physical process involved. Further, we also crudely estimated the oscillator strength and bandwidth (from the ensemble of water configurations around possible cavities), and the results are shown in Figure 5. The quality of the

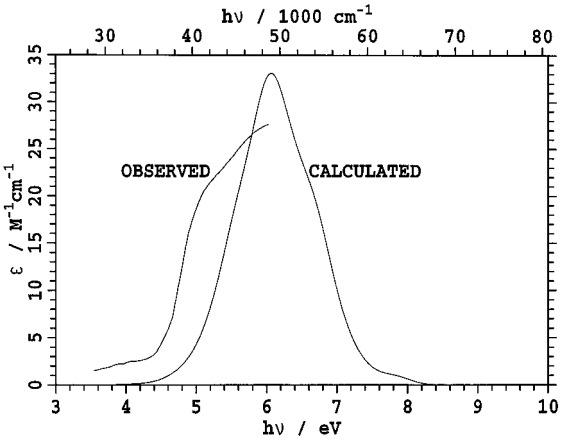

Figure 5. Calculated[52] photoionization spectrum compared to the observed[79] absorption spectrum for aqueous Fe(II). The theoretical spectrum is that predicted for the photoionization of an electron from the complex to preexisting cavities in the water structure.

agreement shown in this figure must be fortuitous, but nevertheless it was concluded that the energy and intensity characteristics of the observed band are

in fact consistent with the photodetachment mechanism. The remaining mechanism that has been proposed is charge transfer to solvent (CTTS). However, present computational capabilities are not yet sufficient for a reliable calculation of such a transition, so that a final answer to the intriguing problem of aqueous Fe(II) is yet to be found. The problem is quite a general one also as very little is known about CTTS processes involving inorganic complexes, and the boundaries (or possibly lack thereof) between orthodox photodetachment and CTTS mechanisms have not been established.

7. Solvent Effect on Metal–Metal Coupling in Dimeric Systems

While a priori calculations using either density-functional or ab initio theory for intramolecular electron-transfer coupling strengths can be made with reasonable accuracy, generally applicable methods for analogous intermetallic couplings are still under construction.[72,73] The quantities of interest are intermetallic coupling strengths for the molecule or ion in solution, so that in addition to other difficulties (e.g., proper treatment of configuration interaction and the difficulty of correctly determining orbital band gaps and positioning metal orbitals within them for the free molecule), there is the problem of accounting for solvent effects. A proper treatment must take into account effects on individual orbitals and transitions and on interference effects. The nature of this problem has been outlined,[72] and some calculations involving diruthenium complexes in which solvent effects on individual orbital levels are calculated using SCIPCM[74] theory have been reported; applications to the bridge dependence of electron transfer in bimetallic porphyrin[73] and polyene[72] complexes have been developed. This problem awaits a more satisfactory resolution, however, and, in principle, all aspects of it may be treated inside the framework of the ZHR−SS approach.

8. Electroabsorption (Stark) Effect

Mention has been made in earlier sections of the measurement of dipole moment change $\Delta\mu$ accompanying an electronic transition. These measurements have been made in the pioneering work of Boxer et al.[22] on the electronic Stark effect in transition metal complexes, which is now being followed up in several laboratories. The original study of Oh, Sano, and Boxer[22] was concerned with the electroabsorption spectra of $Ru^{2+}(NH_3)_5$−pyrazine, Ru^{2+}-$(NH_3)_5$−pyrazine-H^+, the Creutz−Taube ion, and other diruthenium complexes. Other inorganic ruthenium complexes have recently been studied at Brookhaven,[70] and more studies are currently under way in various research laboratories. Basically, these experiments involve the application a very large electric field to a thin sample held dilute in a glass. The theory of Liptay[17] is generally applicable, although, particularly in the case of bimetallic systems with strong intermetallic coupling, modifications are necessary.[75] In addition to the dipole moment change, other quantities such as the change in polarizability and the transition moment hyperpolarizability, are in principle accessible from such measurements. Analyses of typical data can be made either in terms of a model SCF theory[75,76] or by ab initio and semiempirical methods.[50,64] For bimetallic systems, the solvent effect problem outlined in section 7 is a critical one. Nevertheless, the results shown in Table 2 clearly indicate that the ZHR−SS method is appropriate for the quantitative modeling of problems of this type.

9. Conclusions

The ZHR−SS method has provided considerable insight into solvent effects on MLCT and other electronic transitions involving some degree of electron transfer. Its strength lies in its division of a very complicated problem into small units, each of which can be approached individually at the highest feasible level, and the use of reliable perturbation-theory-based methods to describe the somewhat weak inter-unit couplings. Thus, we can employ state of the art ab initio methods to accurately describe the ground and excited states of the chromophore in the gas phase, if necessary, use large simulations with expensive boundary conditions such as Ewald summation to correctly describe the structure of the solvent around the chromophore, and perturbatively evaluate the solvent−solute interaction to determine the solvent effects. Alternate methods which attempt to do all steps at the same time must by necessity introduce severe approximations to the electronic structure of the chromophore and to the liquid structure, and these losses far outweigh the advantages gained by treating the weak solvent−solute interaction nonperturbatively.

Considerable room for improvements to ZHR−SS remain, particularly associated with the desirability of using a consistent high-level ab initio method for determining the electronic structure of the chromophores and linking them into intermolecular potential functions. One aspect of this which has not consistently been properly treated is that the solvent modifies the equilibrium geometry of the solute and that the electronic structure of the solute needs to be evaluated in the gas phase *at the geometry appropriate to the condensed phase*. This effect is particularly important for inorganic complexes for which the relatively weakly held ligands are easily distorted by the solvent. A way to include this is to simply use experimental condensed-phase geometries, but this may not always be possible. An improved version of ZHR−SS could account for this by performing a self-consistent reaction-field calculation for the chromophore not in the gas phase but in some averaged condensed phase. Methods of this type have been shown to be successful in generating intermolecular potential functions[35] and provide for a more general approach in which solvent shifts calculated assuming no specific solvent interactions could be systematically improved.

Calculated solvent shifts for bands which involve a small amount of charge transfer, such as (n,π^*) excitations in azines, fall within 700 cm^{-1} (or ca. 15%) of the experimental values. This error is relatively

large due to the small magnitude of the total effect, and hence it is necessary to consider dispersion and other influences. It is, however, sufficiently small to allow for qualitative interpretation of experimental results and the determination of the key physical properties of the systems. Conversely, in the limit of extensive charge transfer, e.g., for photodetachment transitions in solution, where solvent shifts are 2 orders of magnitude larger, ZHR−SS continues to give useful results. Intermediate between these two limits are MLCT and other intramolecular charge-transfer processes. When the ligand is small (e.g., pyrazine), solvent shifts are on the order of −8000 cm^{-1}, but these would grow in magnitude as the charge separation increased. The accuracy of ab initio calculations for the gas-phase transition energies of these systems, combined with ZHR−SS calculations of the solvent shift, result in transition energies in solution which are in error by ca. 0.5 eV, about twice that regularly obtained by ab initio methods for excitation energies in small organic molecules.

An important application of ZHR−SS has been to understand the results of electroabsorption experiments:[22,70] for MLCT transition in $Ru^{2+}(NH_3)_5$−pyridine and $Ru^{2+}(NH_3)_5$−pyrazine, these depict the transition as moving only one-quarter of an electron from the metal to the ligand and have thus brought into question our physical insight into just what is involved in MLCT excitations. ZHR−SS results have shown that the reduction in the effective number of electrons making the transition is consistent with the view that MLCT involves a one-electron process and that the cloaking of the number of electrons involved arises as the remainder of the system (ligands, other metal orbitals, solvent molecules) combine to minimize the effects of the electronic transition. The numerical results obtained from the simulations vindicate earlier simple analytical models used to describe this effect.[70,76]

10. Acknowledgments

Assistance from the Australian Research Council is gratefully acknowledged.

11. Reference

(1) Born, M. *Z. Phys.* **1920**, *1*, 45.
(2) Booth, F. *J. Chem. Phys.* **1951**, *19*, 391, 1327, 1615.
(3) Kirkwood, J. G. *J. Chem. Phys.* **1939**, *7*, 911.
(4) Gluckauf, E. *Trans. Faraday Soc.* **1964**, *60*, 572.
(5) Bernal, J. D.; Fowler, R. H. *J. Chem. Phys.* **1933**, *1*, 575.
(6) Eley, D. D.; Evans, M. G. *Trans. Faraday Soc.* **1938**, *34*, 1093.
(7) Verwey, E. J. *Recl. Trav. Chim.* **1941**, *60*, 887.
(8) Buckingham, A. D. *Discuss. Faraday Soc.* **1957**, *24*, 151.
(9) Case, B. In *Reactions of Molecules at Electrodes*; Hush, N. S., Ed.; Wiley-Interscience: New York, 1971; p 45.
(10) Bethe, H. *Ann. Phys.* **1929**, *3*, 133.
(11) Griffiths, J. *The Theory of Transition Ions*; Cambridge University Press: London, 1960.
(12) Onsager, L. *J. Am. Chem. Soc.* **1936**, *58*, 1486.
(13) Bayliss, N. S. *J. Chem. Phys.* **1950**, *18*, 292.
(14) McRae, E. G. *J. Phys. Chem.* **1957**, *61*, 562.
(15) Baba, H.; Goodman, L.; Valenti, P. C. *J. Am. Chem. Soc.* **1966**, *88*, 5410.
(16) Levich, V. G. In *Physical Chemistry an Advanced Treatise IX*; Eyring, H., Ed.; Academic: New York, 1970; p 985.
(17) Liptay, W. *Z. Naturforsch. Teil. A* **1965**, *20*, 272.
(18) Rettig, W. *J. Mol. Struct.* **1982**, *84*, 303.
(19) Kasha, M. *Discuss. Faraday Soc.* **1950**, *9*, 14.
(20) Innes, K. K.; Byrne, J. P.; Ross, I. G. *J. Mol. Spectrosc.* **1967**, *22*, 125.
(21) Boxer, S. G.; Goldstein, R. A.; Lockhart, D. J.; Middendorf, T. R.; Takiff, L. *J. Phys. Chem.* **1989**, *93*, 8280.
(22) Oh, D. H.; Sano, M.; Boxer, S. G. *J. Am. Chem. Soc.* **1991**, *113*, 6880.
(23) Bublitz, G. U.; Boxer, S. G. *Annu. Rev. Phys. Chem.* **1997**, *1997*, 213.
(24) Zhou, H.; Boxer, S. G. *J. Phys. Chem. B* **1998**, *102*, 9148.
(25) Bublitz, G. U.; Boxer, S. G. *J. Am. Chem. Soc.* **1998**, *120*, 3988.
(26) Bacskay, G. B.; Reimers, J. R. In *Encyclopaedia of computational chemistry*; Schleyer, P. v. R., Ed.; Wiley: London, 1998; p 2620.
(27) Raineri, F. O.; Resat, H.; Perng, B.-C.; Hirata, F.; Friedman, H. L. *J. Chem. Phys.* **1994**, *100*, 1477.
(28) Karelson, M. M.; Zerner, M. C. *J. Am. Chem. Soc.* **1990**, *112*, 9405.
(29) Karelson, M. M.; Zerner, M. C. *J. Phys. Chem.* **1992**, *96*, 6949.
(30) Ågren, H.; Mikkelsen, K. V. *J. Mol. Struct.* **1991**, *234*, 425.
(31) Klamt, A.; Schüürmann, G. *J. Chem. Soc., Perkin Trans. 2* **1993**, 799.
(32) Dillet, V.; Rinaldi, D.; Rivail, J.-L. *J. Phys. Chem.* **1994**, *98*, 5034.
(33) Cramer, C. J.; Truhlar, D. G. In *Quantitative treatment of solule/solvent interactions*; Politzer, P., Murray, J. S., Eds.; Elsevier: New York, 1994; p 9.
(34) Tomasi, J.; Persico, M. *Chem. Rev.* **1994**, *94*, 2027.
(35) Floris, F.; Persico, M.; Tani, A.; Tomasi, J. *Chem. Phys. Lett.* **1992**, *199*, 518.
(36) Stavrev, K. K.; Zerner, M. C.; Meyer, T. J. *J. Am. Chem. Soc.* **1995**, *117*, 8684.
(37) Broo, A.; Larsson, S. *Chem. Phys.* **1992**, *161*, 363.
(38) Herman, M. F.; Berne, B. J. *J. Chem. Phys.* **1983**, *78*, 4103.
(39) Reimers, J. R.; Wilson, K. R.; Heller, E. J. *J. Chem. Phys.* **1983**, *79*, 4749.
(40) Ilich, P.; Haydock, C.; Prendergast, F. G. *Chem. Phys. Lett.* **1989**, *158*, 129.
(41) Levy, R. M.; Westbrook, J. D.; Kitchen, D. B.; Krogh-Jespersen, K. *J. Phys. Chem.* **1991**, *95*, 6756.
(42) Aqvist, J.; Warshel, A. *Chem. Rev.* **1993**, *93*, 2523.
(43) Muiño, P. L.; Callis, P. R. *J. Chem. Phys.* **1994**, *100*, 4093.
(44) Thiel, W. *Adv. Chem. Phys.* **1996**, *XCIII*, 703.
(45) Tuckerman, M.; Laasonen, K.; Sprik, M.; Parrinello, M. *J. Chem. Phys.* **1995**, *103*, 150.
(46) Luzhkov, V.; Warshel, A. *J. Am. Chem. Soc.* **1991**, *113*, 4491.
(47) DeBolt, S. E.; Kollman, P. A. *J. Am. Chem. Soc.* **1990**, *112*, 7515.
(48) Zeng, J.; Hush, N. S.; Reimers, J. R. *J. Am. Chem. Soc.* **1996**, *118*, 2059.
(49) Basilevsky, M. V.; Rostov, I. V.; Newton, M. D. *Chem. Phys.* **1998**, *232*, 189.
(50) Zeng, J.; Hush, N. S.; Reimers, J. R. *J. Phys. Chem.* **1996**, *100*, 19292.
(51) Rullmann, J. A. C.; van Duijnen, P. Th. *Mol. Phys.* **1987**, *61*, 293.
(52) Zeng, J.; Craw, J. S.; Hush, N. S.; Reimers, J. R. *J. Phys. Chem.* **1994**, *98*, 11075.
(53) Zeng, J.; Hush, N. S.; Reimers, J. R. *J. Chem. Phys.* **1993**, *99*, 1508.
(54) Zeng, J.; Hush, N. S.; Reimers, J. R. *J. Phys. Chem.* **1995**, *99*, 10459.
(55) Friedman, H. L. *Mol. Phys.* **1975**, *29*, 1533.
(56) Zeng, J.; Craw, J. S.; Hush, N. S.; Reimers, J. R. *J. Chem. Phys.* **1993**, *99*, 1482.
(57) Singh, U. C.; Brown, F. K.; Bash, P. A.; Kollman, P. A. *J. Am. Chem. Soc.* **1987**, *109*, 1607.
(58) Cieplak, P.; Kollman, P. A. *J. Am. Chem. Soc.* **1988**, *110*, 3734.
(59) Weiner, S. J.; Kollman, P. A.; Case, D. A.; Singh, U. C.; Ghio, C.; Alagona, G.; Profeta, S., Jr.; Weiner, P. *J. Am. Chem. Soc.* **1984**, *106*, 765.
(60) Weiner, S. J.; Kollman, P. A.; Nguyen, D. T.; Case, D. A. *J. Comput. Chem.* **1986**, *7*, 230.
(61) Zeng, J.; Woywod, C.; Hush, N. S.; Reimers, J. R. *J. Am. Chem. Soc.* **1995**, *117*, 8618.
(62) Comba, P.; Hambley, T. *Molecular modelling of inorganic systems*; VCH: Weinheim, 1995.
(63) Zeng, J.; Hush, N. S.; Reimers, J. R. *J. Chem. Phys.* **1993**, *99*, 1495.
(64) Zeng, J.; Hush, N. S.; Reimers, J. R. *J. Phys. Chem.* **1996**, *100*, 9561.
(65) Reimers, J. R.; Hush, N. S. *Chem. Phys.* **1996**, *208*, 177.
(66) Jorgensen, W. L.; Chandrasekhar, J.; Madura, J. D.; Impey, R. W.; Klein, M. L. *J. Chem. Phys.* **1983**, *79*, 926.
(67) Broo, A. *Chem. Phys.* **1993**, *174*, 127.
(68) Zhang, L.-T.; Ondrechen, M. J. *Inorg. Chim. Acta* **1994**, *226*, 43.
(69) Magnuson, R. H.; Taube, H. *J. Am. Chem. Soc.* **1975**, *97*, 5129.
(70) Shin, Y. K.; Brunschwig, B. S.; Creutz, C.; Sutin, N. *J. Phys. Chem.* **1996**, *100*, 8157.
(71) Zeng, J.; Craw, J. S.; Hush, N. S.; Reimers, J. R. *Chem. Phys. Lett.* **1993**, *206*, 323.
(72) Reimers, J. R.; Hush, N. S. *J. Phys. Chem. A* **1999**, *103*, 3066.

(73) Hush, N. S.; Reimers, J. R.; Hall, L. E.; Johnston, L. A.; Crossley, M. J. *Ann. N.Y. Acad. Sci.* **1998**, *852*, 1.
(74) Cossi, M.; Barone, V.; Cammi, R.; Tomasi, J. *Chem. Phys. Lett.* **1996**, *255*, 327.
(75) Reimers, J. R.; Hush, N. S. In *Mixed Valence Systems: Applications in Chemistry, Physics, and Biology*; Prassides, K., Ed.; Kluwer Academic Publishers: Dordrecht, 1991; p 29.
(76) Reimers, J. R.; Hush, N. S. *J. Phys. Chem.* **1991**, *95*, 9773.
(77) Spencer, N. N.; Holmboe, E. S.; Kirshenbaum, M. R.; Barton, S. W.; Smith, K. A.; Wolbach, W. S.; Powell, J. F.; Chorazy, C. *Can. J. Chem.* **1982**, *60*, 1184.
(78) Kleier, D. A.; Martin, R. L.; Wadt, W. R.; Moomaw, W. R. *J. Am. Chem. Soc.* **1982**, *104*, 60.
(79) Rigg, T.; Weiss, J. *J. Chem. Phys.* **1952**, *20*, 1194.

CR980409V